

Electronic Structure Calculation of Graphene by Formulating a Relativistic Tight-Binding Model

Rohin Sharma^{1,*}, Dipendra B. Hamal¹, Amit Shrestha², Katsuhiko Higuchi²

April 15, 2022

¹ *Department of Physics, Kathmandu University, Dhulikhel, Nepal.*

² *Graduate School of Advanced Science of Matter, Hiroshima University, Higashi-Hiroshima 739-8527, Japan.*

* rohin.sharma.1993@gmail.com

Keywords: MFRTB method, TB approximation,

A non-perturbative relativistic tight-binding (TB) approximation method applicable to crystalline material immersed in magnetic field was developed in 2015 [1]. To apply this method to any material in magnetic field, the electronic structure of the material in absence of magnetic field must be calculated. In this study, we present the relativistic TB approximation method for graphene in zero magnetic field. The Hamiltonian and overlap matrix is constructed considering the nearest neighbouring atomic interactions between the s and p valence orbitals, where the relativistic hopping and overlap integrals are calculated using the relativistic version of the Slater-Koster table. The method of constructing the Hamiltonian and overlap matrix and the resulting energy-band structure of graphene in the first Brillouin zone is presented in this paper. It is found that there is an appearance of a small band-gap at the K points (also known as the spin-orbit gap) due to the relativistic effect, whose magnitude is $25 \mu\text{eV}$.

1 Introduction

The popularity in graphene research mainly stems from its unique and fascinating electronic [2, 3, 4, 5] and magnetic properties [5, 6, 7] and also due to the promise of potential applications and emergence of a new paradigm of relativistic-condensed matter physics [8]. Some of these physical properties are: it's minimum conductance never falls below the value corresponding to the smallest quantum unit of conductance even when the charge carrier concentrations tends to zero [2], tunable conductivity in twisted monolayer-bilayer graphene system [5], insulating behaviour at low temperatures [5], half-integer quantum hall effect [7], unconventional magnetic oscillations [9] and strong orbital diamagnetism [10]. The anomalous electronic properties of graphene arises from its characteristic band structure which is due to the effectively massless charge carriers with relativistic behaviour known as Dirac fermions at energies near Fermi level where the conical valance band and conduction band meet at a single point in momentum space called the Dirac points.

Because of these physical properties of graphene it is desirable to investigate into a first principle calculation method that takes into account both the relativistic effect and magnetic field. There are several studies where the electronic structure is calculated with non-relativistic tight binding model [11, 12] and a large

number of these studies have been without considering the overlap integral [12, 13, 4]. There also exists a lot of credible relativistic calculation methods of electronic structures in absence of magnetic field [14, 15, 16] that have been successfully applied to f-electron materials [17], but the electronic structure calculation method that can deal with magnetic field and relativistic effects simultaneously is desired for the study.

In 2015 a Non-perturbative Tight-Binding (TB) method called the magnetic-field-containing relativistic tight-binding approximation method (MFRTB method) was developed incorporating both the relativistic effects and magnetic field in the same footing and was applied to silicon crystal immersed in magnetic field [1]. The MFRTB method was developed to alternatively describe the oscillatory behaviour of the magnetization as a function of magnetic field (the de Haas-van Alphen effect) from a view point of the first-principle calculation. The MFRTB method was successfully able to calculate the relativistic energy band structures of silicon in an external magnetic field [1] that explained the suppression of softening in the elastic constant of boron-doped silicon in an external magnetic field, and also revisit the dHvA effect in a first-principle way [18]. This method also presents the relativistic version of the Slater-Koster table in which the relativistic hopping integrals are explicitly expressed in terms of relativistic TB parameters for the interactions corresponding to $2s$ and $2p$ orbitals.

In order to apply the MFRTB method to graphene in magnetic field, the magnetic hopping integrals must be expressed in terms of relativistic hopping integrals for zero magnetic field and magnetic field-dependent phase factor. So as an initial step, we need to formulate a relativistic TB approximation method for graphene in zero magnetic field. In this paper a relativistic TB model for graphene in absence of magnetic field is formulated starting from the Dirac equation for an electron in a periodic potential. Then the Dirac hamiltonian matrix and overlap matrix of the system is constructed utilizing the relativistic Slater-Koster table considering the nearest neighbour interactions between $2s$ and $2p$ orbitals. Then by solving the general eigen value equation for different \mathbf{k} points in the first Brillouin zone using computer program (Python), the relativistic electronic structure of graphene is produced. Our results have shown an appearance of a small band gap ($25 \mu\text{eV}$) at the Dirac points due to the relativistic effect (spin-orbit coupling), which is in excellent agreement with the first principle calculation results using the linearized augmented plane-wave method incorporating the spin-orbit coupling [19].

2 Relativistic TB theory for graphene lattice in zero magnetic field

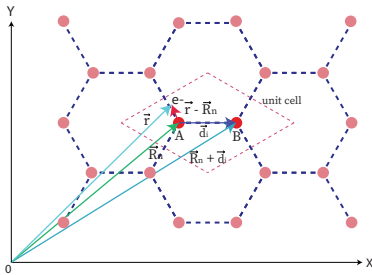


Figure 1: Illustration of honeycomb lattice and unit cell of graphene

Considering the two atoms of the unit cells of the honeycomb lattice, we proceed to establish the equations for the hamiltonian matrix elements and the overlap matrix elements of the system. We represent the two atoms of the unit cell as ‘A’ and ‘B’.

2.1 For lattice site ‘A’

The Dirac equation for an electron at lattice site ‘A’ is

$$\hat{H}_A \Psi_{\alpha, \vec{k}}(\vec{r}) = E(\vec{k}) \Psi_{\alpha, \vec{k}}(\vec{r}), \quad (1)$$

with the atomic hamiltonian at site ‘A’ as

$$\hat{H}_A = c\vec{\alpha} \cdot \vec{p} + \beta mc^2 + V_A(\vec{r} - \vec{R}_n). \quad (2)$$

where c denote the velocity of light, m denote the electron rest mass, $\vec{\alpha} = (\alpha_x, \alpha_y, \alpha_z)$, β stands for the

usual 4×4 matrices [20], $V_A(\vec{r} - \vec{R}_n)$ represents the Coulomb potential due to the nucleus of atom at site ‘A’ located at \vec{R}_n , the subscripts α and \vec{k} of the eigen function $\Psi_{\alpha, \vec{k}}(\vec{r})$ represents the band index and crystal momentum respectively.

Expanding $\Psi_{\alpha, \vec{k}}(\vec{r})$ by using the Bloch sum of relativistic atomic orbital $\phi_{nlJM}^A(\vec{r})$ of atom at ‘A’ as the basis function, we have

$$\Psi_{\alpha, \vec{k}}(\vec{r}) = \sum_{nlJM} C_{nlJM, \vec{K}}^A B_{nlJM}^A(\vec{r}), \quad (3)$$

where $C_{nlJM, \vec{K}}^A$ is the expansion coefficient and $B_{nlJM}^A(\vec{r})$ denote the Bloch sum which is written as

$$B_{nlJM}^A(\vec{r}) = \frac{1}{\sqrt{N}} \sum_{\vec{R}_n} e^{i\vec{k} \cdot \vec{R}_n} \phi_{nlJM}(\vec{r} - \vec{R}_n). \quad (4)$$

The n, l, M and J in Eq. (4) are the principle, angular momentum, total angular momentum and magnetic quantum numbers respectively. Here the relativistic atomic orbital obeys the following Dirac equation;

$$[c\vec{\alpha} \cdot \vec{p} + \beta mc^2 + V_A(\vec{r} - \vec{R}_n)] \phi_{nlJM}(\vec{r} - \vec{R}_n) = \varepsilon_{nlJ}^A \phi_{nlJM}(\vec{r} - \vec{R}_n) \quad (5)$$

where ε_{nlJ}^A denotes the atomic spectrum for zero magnetic field and is independent of M .

In Eq. (1) multiplying by $\phi_{n'l'J'M'}^{\dagger A'}(\vec{r} - \vec{R}_{n'})$ where $\vec{R}_{n'} \neq \vec{R}_n$, $A' \neq A$ and integrating and denoting the hopping and overlap integrals by $t_{n'l'J'M', nlJM}^{A'A}(\vec{R}_n - \vec{R}_{n'})$ and $s_{n'l'J'M', nlJM}^{A'A}(\vec{R}_n - \vec{R}_{n'})$ respectively, we define the hamiltonian and overlap matrix elements as

$$\begin{aligned} \mathbf{H}_{n'l'J'M', nlJM}^{A'A}(\vec{K}) &= \sum_{\vec{R}_n} e^{i\vec{k} \cdot \vec{R}_n} t_{n'l'J'M', nlJM}^{A'A}(\vec{R}_n - \vec{R}_{n'}), \\ & \end{aligned} \quad (6)$$

and,

$$\begin{aligned} \mathbf{S}_{n'l'J'M', nlJM}^{A'A}(\vec{K}) &= \sum_{\vec{R}_n} e^{i\vec{k} \cdot \vec{R}_n} s_{n'l'J'M', nlJM}^{A'A}(\vec{R}_n - \vec{R}_{n'}). \\ & \end{aligned} \quad (7)$$

So Eq. (1) becomes

$$\sum_{nlJM} \mathbf{H}_{n'l'J'M', nlJM}^{A'A}(\vec{K}) C_{nlJM, \vec{K}}^A = E(\vec{K}) \sum_{nlJM} \mathbf{S}_{n'l'J'M', nlJM}^{A'A}(\vec{K}) C_{nlJM, \vec{K}}^A \quad (8)$$

After evaluating the relativistic hopping and overlap integrals when the lattice site is considered to be at the origin ($\vec{R}_n = 0, d_i = d_j$) and when the lattice site is considered to be elsewhere ($\vec{R}_n \neq 0, d_i \neq d_j$) and by neglecting the three center integral, we get the matrix elements of the hamiltonian and overlap Eq. (6) and Eq. (7) as:

$$\begin{aligned} \mathbf{H}_{n'l'J'M',nlJM}^{A'A}(\vec{K}) = & \\ & (\varepsilon_{nlJ}^A + \Delta\varepsilon_{nlJM}^A)\delta_{n'l'J'M',nlJM}\delta_{i,j} \\ & + \sum_{\vec{R}_n} e^{i\vec{k}\cdot\vec{R}_n} (1 - \delta_{\vec{R}_n,0}\delta_{i,j}) t_{n'l'J'M',nlJM}^{new,A'A}(\vec{R}_n), \end{aligned} \quad (9)$$

with

$$\begin{aligned} t_{n'l'J'M',nlJM}^{new,A'A}(\vec{R}_n) = & \\ & \frac{1}{2}(\varepsilon_{nlJ}^A + \varepsilon_{n'l'J'}^A) s_{n'l'J'M',nlJM}^{A'A}(\vec{r} - \vec{R}_n) \\ & + \int \phi_{n'l'J'M'}^{\dagger A'}(\vec{r}) \left(\frac{V_{A'}(\vec{r}) + V_A(\vec{r} - \vec{R}_n)}{2} \right) \\ & \times \phi_{nlJM}^A(\vec{r} - \vec{R}_n) d^3\vec{r}, \end{aligned} \quad (10)$$

and

$$\begin{aligned} \mathbf{S}_{n'l'J'M',nlJM}^{A'A}(\vec{K}) = & \delta_{n'l'J'M',nlJM}\delta_{i,j} \\ & + \sum_{\vec{R}_n} e^{i\vec{k}\cdot\vec{R}_n} (1 - \delta_{\vec{R}_n,0}\delta_{i,j}) s_{n'l'J'M',nlJM}^{A'A}(\vec{R}_n), \end{aligned} \quad (11)$$

with

$$s_{n'l'J'M',nlJM}^{A'A}(\vec{R}_n) = \int \phi_{n'l'J'M'}^{\dagger A'}(\vec{r}) \phi_{nlJM}^A(\vec{r} - \vec{R}_n) d^3\vec{r}. \quad (12)$$

In Eq. (9) $\Delta\varepsilon_{nlJM}^A$ denotes the crystal field energy due to the influence of other lattice sites on site 'A' written as:

$$\begin{aligned} \Delta\varepsilon_{nlJM}^A = & \int \phi_{n'l'J'M'}^{\dagger A'}(\vec{r}) \sum_{\vec{R}_m \neq \vec{R}_n} \sum_{A' \neq A} V_A(\vec{r} - \vec{R}_m) \\ & \times \phi_{nlJM}^A(\vec{r} - \vec{R}_m) d^3\vec{r}. \end{aligned} \quad (13)$$

2.2 For lattice site 'B'

Similarly for Lattice site 'B' located at $\vec{R}_n + \vec{d}_i$ where \vec{d}_i is the position vector from 'A' to 'B', we can formulate the hamiltonian and overlap matrix elements as:

$$\begin{aligned} \mathbf{H}_{n'l'J'M',nlJM}^{B'B}(\vec{K}) = & \\ & (\varepsilon_{nlJ}^B + \Delta\varepsilon_{nlJM}^B)\delta_{n'l'J'M',nlJM}\delta_{i,j} \\ & + \sum_{\vec{R}_n} e^{i\vec{k}\cdot(\vec{R}_n + \vec{d}_i)} (1 - \delta_{\vec{R}_n,0}\delta_{i,j}) \\ & \times t_{n'l'J'M',nlJM}^{B'B,new}(\vec{R}_n - \vec{d}_i + \vec{d}_j). \end{aligned} \quad (14)$$

with

$$\begin{aligned} t_{n'l'J'M',nlJM}^{B'B,new}(\vec{R}_n - \vec{d}_i + \vec{d}_j) = & \\ & \frac{1}{2}(\varepsilon_{n'l'J'}^B + \varepsilon_{nlJ}^B) s_{n'l'J'M',nlJM}^{B'B}(\vec{r} - \vec{R}_n - \vec{d}_i + \vec{d}_j) \\ & + \int \phi_{n'l'J'M'}^{\dagger B'}(\vec{r}) \frac{V_{B'}(\vec{r}) + V_B(\vec{r} - \vec{R}_n - \vec{d}_i + \vec{d}_j)}{2} \\ & \times \phi_{nlJM}^B(\vec{r} - \vec{R}_n - \vec{d}_i + \vec{d}_j) d^3\vec{r}, \end{aligned} \quad (15)$$

and

$$\begin{aligned} \mathbf{S}_{n'l'J'M',nlJM}^{B'B}(\vec{K}) = & \delta_{n'l'J'M',nlJM}\delta_{i,j} \\ & + \sum_{\vec{R}_n} e^{i\vec{k}\cdot(\vec{R}_n + \vec{d}_i)} (1 - \delta_{\vec{R}_n,0}\delta_{i,j}) \\ & \times s_{n'l'J'M',nlJM}(\vec{R}_n - \vec{d}_i + \vec{d}_j) \end{aligned} \quad (16)$$

with

$$\begin{aligned} s_{n'l'J'M',nlJM}^{B'B}(\vec{R}_n - \vec{d}_i + \vec{d}_j) = & \\ = & \int \phi_{n'l'J'M'}^{\dagger B'}(\vec{r}) \phi_{nlJM}^B(\vec{r} - \vec{R}_n - \vec{d}_i + \vec{d}_j) d^3\vec{r}. \end{aligned} \quad (17)$$

In Eq. (14) the crystal field energy $\Delta\varepsilon_{nlJM}^B$ due to the influence of other lattice sites on site 'B' is written as:

$$\begin{aligned} \Delta\varepsilon_{nlJM}^B = & \int \phi_{n'l'J'M'}^{\dagger B'}(\vec{r}) \sum_{\vec{R}_m \neq \vec{R}_n} \sum_{B' \neq B} V_{B'}(\vec{r} - \vec{R}_m - \vec{d}_j) \\ & \times \phi_{nlJM}^B(\vec{r} - \vec{R}_m - \vec{d}_j) d^3\vec{r}. \end{aligned} \quad (18)$$

2.3 Hamiltonian and overlap matrix elements of the system

According to Eq. (9) and Eq. (14), the equations of hamiltonian matrix elements for site 'A' and 'B' differs only in the position of lattice sites, so we can formulate a general form of hamiltonian and overlap matrix elements considering the nearest neighbouring interactions in a graphene lattice as,

$$\begin{aligned} \mathbf{H}_{n'l'J'M',nlJM}(\vec{K}) = & \\ & (\varepsilon_{nlJ} + \Delta\varepsilon_{nlJM})\delta_{n'l'J'M',nlJM}\delta_{i,j} \\ & + (1 - \delta_{\vec{R}_n,0}\delta_{i,j}) \sum_{\vec{R}_n} \sum_{i=1}^3 e^{i\vec{k}\cdot(\vec{R}_n + \vec{d}_i)} \\ & \times t_{n'l'J'M',nlJM}^{new}(\vec{R}_n - \vec{d}_i + \vec{d}_j). \end{aligned} \quad (19)$$

and

$$\begin{aligned} \mathbf{S}_{n'l'J'M',nlJM}(\vec{K}) = & \delta_{n'l'J'M',nlJM}\delta_{i,j} \\ & + (1 - \delta_{\vec{R}_n,0}\delta_{i,j}) \sum_{\vec{R}_n} \sum_{i=1}^3 e^{i\vec{k}\cdot(\vec{R}_n + \vec{d}_i)} \\ & \times s_{n'l'J'M',nlJM}(\vec{R}_n - \vec{d}_i + \vec{d}_j). \end{aligned} \quad (20)$$

Here the values of i goes from 1 to 3 because there are 3 nearest neighbours for any atom in a honeycomb lattice of graphene and \vec{d}_i represents their position vectors. The superscripts 'A' and 'B' are eliminated because both are carbon atoms.

Then Eq.(8) is rewritten as:

$$\begin{aligned}
& \sum_{nlJM} [(\varepsilon_{nlJ} + \Delta\varepsilon_{nlJM})\delta_{n'l'J'M',nlJM} \\
& + \sum_{\vec{R}_n} \sum_{i=1}^3 e^{i\vec{k}\cdot(\vec{R}_n+\vec{d}_i)} (1 - \delta_{\vec{R}_n,0}\delta_{i,j}) \\
& t_{n'l'J'M',nlJM}^{new}(\vec{R}_n - \vec{d}_i + \vec{d}_j)] C_{nlJM,\vec{k}}^i \quad (21) \\
& = E(\vec{k})[\delta_{n'l'J'M',nlJM}\delta_{i,j} \\
& + \sum_{\vec{R}_n} \sum_{i=1}^3 e^{i\vec{k}\cdot(\vec{R}_n+\vec{d}_i)} (1 - \delta_{\vec{R}_n,0}\delta_{i,j}) \\
& \times s_{n'l'J'M',nlJM}^{ij}(\vec{R}_n - \vec{d}_i + \vec{d}_j)] C_{nlJM,\vec{k}}^i
\end{aligned}$$

Eq. (21) is called the simultaneous equation which needs to be solved to obtain the energy eigen value $E(\vec{k})$.

3 Method

3.1 Construction of hamiltonian and overlap matrix of the system

In our calculations, we have considered the atomic states of valance orbitals of carbon atom so the interactions takes place among the following 8 atomic states: $(2, 0, \frac{1}{2}, \frac{1}{2})$, $(2, 0, \frac{1}{2}, -\frac{1}{2})$, $(2, 1, \frac{1}{2}, \frac{1}{2})$, $(2, 1, \frac{3}{2}, \frac{1}{2})$, $(2, 1, \frac{1}{2}, -\frac{1}{2})$, $(2, 1, \frac{3}{2}, -\frac{1}{2})$, $(2, 1, \frac{3}{2}, \frac{3}{2})$ and $(2, 1, \frac{3}{2}, -\frac{3}{2})$.

We can now construct the Hamiltonian and overlap matrix using Eq. (19) and Eq. (20). To obtain the numerical values of $t_{n'l'J'M',nlJM}^{new}(\vec{R}_n - \vec{d}_i + \vec{d}_j)$ and $s_{n'l'J'M',nlJM}^{new}(\vec{R}_n - \vec{d}_i + \vec{d}_j)$ we have used the relativistic version of the Slater-Koster table [1] to express hopping and overlap integrals in terms of the TB parameters $K_d^{i,j}(n'l'J',nlJ)_{|M|}$ and $S_d^{i,j}(n'l'J',nlJ)_{|M|}$ and then solving Eq. (10) and Eq. (11). Since the crystal field energy is very small compared to the atomic spectrum, we have neglected $\Delta\varepsilon_{nlJM}$ and used the atomic spectrum ε_{nlJ} that is calculated using density functional theory [21, 22] based on local density approximation [23]. The numerical values of the term $\varepsilon_{nlJ} + \Delta\varepsilon_{nlJM}$ are listed in Table (1). The numerical values of the TB parameters for the 8 atomic states of the nearest neighbouring atoms of graphene $K_1(n'l'J',nlJ)_{|M|}$ and $S_1(n'l'J',nlJ)_{|M|}$ has been calculated [23] which are listed in Table (2).

Table 1: Numerical values of the sum of electronic spectra and crystal field energy[23].

Energy States	Numerical values (eV)
$\varepsilon_{20\frac{1}{2}} + \Delta\varepsilon_{20\frac{1}{2}M}$	-8.37
$\varepsilon_{21\frac{1}{2}} + \Delta\varepsilon_{21\frac{1}{2}M}$	0
$\varepsilon_{21\frac{3}{2}} + \Delta\varepsilon_{21\frac{3}{2}M}$	8.305×10^{-3}

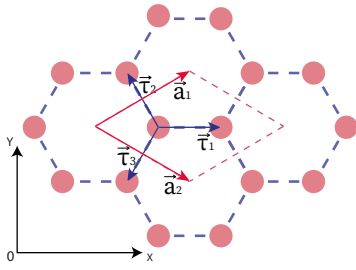
Table 2: Relativistic TB parameters for the hopping and overlap integrals for nearest neighbouring graphene atoms.

$(nlJM)$	Numerical values (eV)
$K_1(20\frac{1}{2}, 20\frac{1}{2})_{\frac{1}{2}}$	-5.727
$K_1(20\frac{1}{2}, 21\frac{1}{2})_{\frac{1}{2}}$	-3.226
$K_1(20\frac{1}{2}, 21\frac{3}{2})_{\frac{1}{2}}$	4.587
$K_1(21\frac{1}{2}, 21\frac{1}{2})_{\frac{1}{2}}$	-1.81×10^{-2}
$K_1(21\frac{1}{2}, 21\frac{3}{2})_{\frac{1}{2}}$	-4.298
$K_1(21\frac{3}{2}, 21\frac{3}{2})_{\frac{1}{2}}$	3.01
$K_1(21\frac{3}{2}, 21\frac{3}{2})_{\frac{3}{2}}$	-3.064
$S_1(20\frac{1}{2}, 20\frac{1}{2})_{\frac{1}{2}}$	1.012×10^{-1}
$S_1(20\frac{1}{2}, 21\frac{1}{2})_{\frac{1}{2}}$	9.739×10^{-2}
$S_1(20\frac{1}{2}, 21\frac{3}{2})_{\frac{1}{2}}$	-1.392×10^{-1}
$S_1(21\frac{1}{2}, 21\frac{1}{2})_{\frac{1}{2}}$	-7.904×10^{-2}
$S_1(21\frac{1}{2}, 21\frac{3}{2})_{\frac{1}{2}}$	2.081×10^{-1}
$S_1(21\frac{3}{2}, 21\frac{3}{2})_{\frac{1}{2}}$	-2.289×10^{-1}
$S_1(21\frac{3}{2}, 21\frac{3}{2})_{\frac{3}{2}}$	6.802×10^{-2}

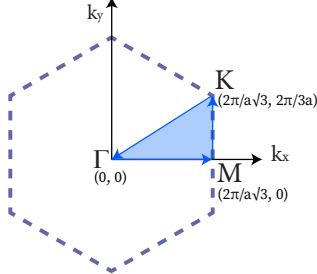
By utilizing the values from Table (1) and Table (2) and using Eq. (19) and Eq. (20) for the 8 atomic states at sites 'A', 'B' and 'A'', 'B'', a 16×16 hamiltonian and overlap matrix is constructed. The first term of Eq. (19) and Eq. (20) vanishes for the non-diagonal diagonal elements (since $n'l'J'M' \neq nlJM$ and $i \neq j$), the second term vanishes for the diagonal elements (since $i = j$ and $\vec{R}_n = 0$). The tabular representation of thus-constructed hamiltonian and overlap matrix is shown in the Appendix section.

3.2 Electronic structure calculation

The real and reciprocal lattice of honeycomb graphene lattice along with the position coordinates of the high symmetry points are shown in figures below.



(a) Illustration of real lattice and unit cell of graphene.



(b) Illustration of reciprocal lattice and first Brillouin zone of graphene.

Figure 2: Illustration of graphene lattice in real and reciprocal space.

It can be shown that the position coordinates of the high symmetry points are as follows:

$$\begin{aligned}
 \Gamma &= (0, 0) \\
 K &= \left(\frac{2\pi}{a\sqrt{3}}, \frac{2\pi}{3a} \right) \\
 M &= \left(\frac{2\pi}{a\sqrt{3}}, 0 \right)
 \end{aligned} \tag{22}$$

After we have constructed the Hamiltonian and overlap matrix of graphene, we can solve the general eigen value Eq. (8) to get the energy eigen value $E(\vec{k})$, and since the energy eigen value is a function of \vec{k} we need to solve the eigen value equation along the high symmetry points in the \vec{k} -space along a closed contour to obtain a continuous electronic band structure. For our calculation, the contour of $K - \Gamma - M - K$ is chosen.

3.3 Computing Algorithm

The necessary computations were done in Python 3.8.5 utilizing python libraries. The following libraries were used in our calculation. “linalg” was imported from the “scipy” library to carryout the eigen value problem calculation. “numpy” and “math” libraries were used to create matrix and to perform mathematical calculations. “Matplotlib” was used to generate the plots of energy eigenvalues with respect to k points.

After assigning the variables for each matrix elements of the top right 8×8 submatrices of the hamiltonian (Table 3) and overlap matrix (Table 4) and the diagonal elements, we constructed the matrices using the command “numpy.array”. Then the general eigenvalue

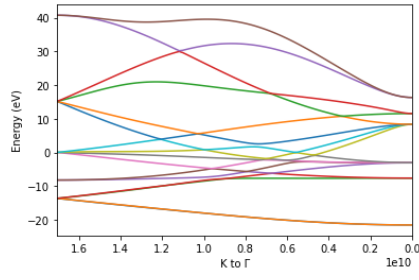
equation was solved by utilizing the linear algebra package “linalg” and the eigen values are stored in a variable. `cmd-line: lamda=linalg.eigh(H,S,lower=False)`

In order to calculate the eigenvalues along the contour defined above, each path from $K - \Gamma - M - K$ was divided into 100 equal intervals including the starting and the end points using the command “numpy.linspace”. A list of equally spaced numbers from the coordinates of K to coordinates of Γ , from coordinates of Γ to coordinates of M and from coordinates of M back to coordinates of K were generated as \vec{k} points representing the X-axis. Then by using the “for” loop, the eigenvalue equation was solved for each of the \vec{k} points in the interval. The corresponding eigenvalues were stored in a new list, which was plotted against the k points interval to get the desired electronic band structure. The band gap value was calculated by taking the energy difference between the highest occupied and the lowest unoccupied state at the \vec{k} point corresponding to the coordinates of symmetry point K .

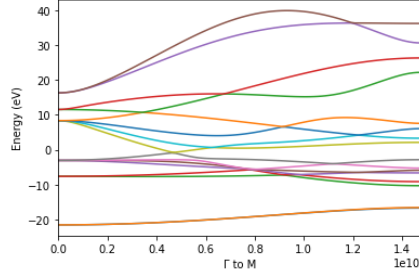
4 Result

The obtained band gap energy at the K point was $2.5832076860657534 \times 10^{-5}$ eV whose value is in close agreement with the value shown by the first-principle calculations considering spin-orbit interaction done by the FLAPW method [19].

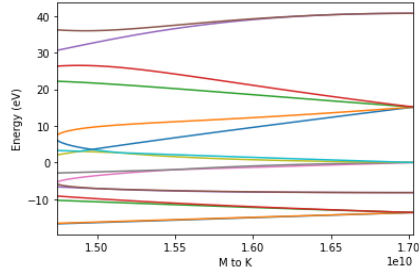
The figures below shows the energy band diagrams obtained from the above mentioned algorithm.



(a) Energy bands from K to Γ

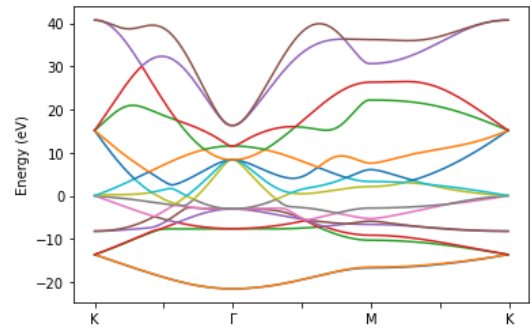


(b) Energy bands from Γ to M

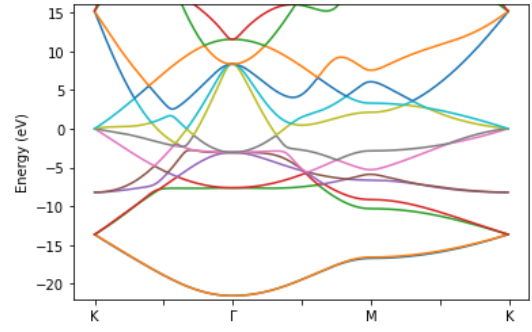


(c) Energy bands from M to K

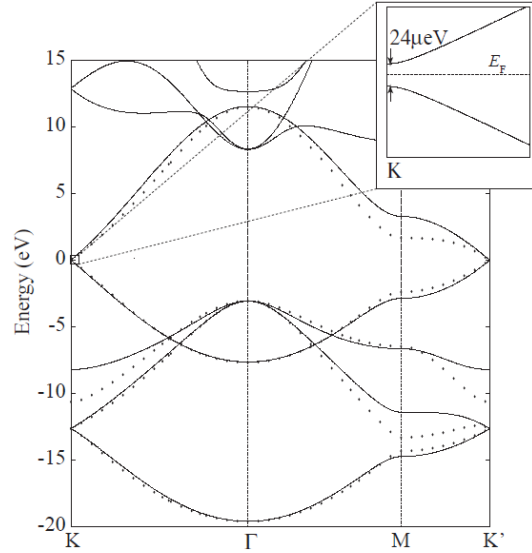
Figure 3: Energy bands obtained at different k point intervals.



(a) Energy bands of graphene.



(b) Enlarged view of the energy bands.



(c) Reference energy band structure of graphene by the wien2k code [23].

Figure 4: Relativistic energy bands structure of graphene.

4.1 Remarks and conclusion

- (i) We have developed the relativistic tight-binding model that enables us to calculate the electronic structure and electronic properties of graphene, taking into account the relativistic effects by treating the Dirac equation for electron moving in a periodic potential.
- (ii) The formulation is accomplished in the orthodox coordinate representation.
- (iii) Using the general expressions to calculate the

The energy diagram obtained from the calculation along the closed contour $K - \Gamma - M - K$ is shown in Fig. (4a) and Fig.(4b) below. The reference data using the FLAPW method is shown in Fig. (4c).

Hamiltonian and overlap matrix, we have constructed the Dirac Hamiltonian and overlap matrix of the system considering the nearest neighbouring atomic interactions.

- (iv) By solving the general eigenvalue equation for different \vec{k} points, we have successfully revealed the relativistic electronic band structure of graphene.
- (v) Appearance of a small energy band gap due to the spin-orbit interaction, along with the energy band-gap value has been shown.

The validity of the MFRTB method has been successfully tested and the magnetic field effects can also be

incorporated into the present model by utilizing magnetic Bloch theorem and approximating the magnetic hopping integrals as the relativistic hopping integrals multiplied by the magnetic-field-dependent phase factor, which would be our future works. In conclusion, this is a coherent relativistic tight-binding model that can be applied to accurately predict the relativistic effects for various systems.

5 Acknowledgement

This work was supported by the Department of Physics, Kathmandu University, Dhulikhel, Nepal.

6 Appendix

Table 3: Hamiltonian matrix representation in tabular form.

\times	A								B							
	$(2,0,\frac{1}{2},\frac{1}{2})$	$(2,0,\frac{1}{2},-\frac{1}{2})$	$(2,1,\frac{1}{2},\frac{1}{2})$	$(2,1,\frac{1}{2},-\frac{1}{2})$	$(2,1,\frac{3}{2},\frac{3}{2})$	$(2,1,\frac{3}{2},\frac{1}{2})$	$(2,1,\frac{3}{2},-\frac{1}{2})$	$(2,1,\frac{3}{2},-\frac{3}{2})$	$(2,0,\frac{1}{2},\frac{1}{2})$	$(2,0,\frac{1}{2},-\frac{1}{2})$	$(2,1,\frac{1}{2},\frac{1}{2})$	$(2,1,\frac{1}{2},-\frac{1}{2})$	$(2,1,\frac{3}{2},\frac{3}{2})$	$(2,1,\frac{3}{2},\frac{1}{2})$	$(2,1,\frac{3}{2},-\frac{1}{2})$	$(2,1,\frac{3}{2},-\frac{3}{2})$
$(2,0,\frac{1}{2},\frac{1}{2})$	$a_{1,1}$	0	0	0	0	0	0	0	$a_{1,9}$	$a_{1,10}$	$a_{1,11}$	$a_{1,12}$	$a_{1,13}$	$a_{1,14}$	$a_{1,15}$	$a_{1,16}$
$(2,0,\frac{1}{2},-\frac{1}{2})$	0	$a_{2,2}$	0	0	0	0	0	$a_{2,9}$	$a_{2,10}$	$a_{2,11}$	$a_{2,12}$	$a_{2,13}$	$a_{2,14}$	$a_{2,15}$	$a_{2,16}$	$a_{2,17}$
$(2,1,\frac{1}{2},\frac{1}{2})$	0	0	$a_{3,3}$	0	0	0	0	$a_{3,9}$	$a_{3,10}$	$a_{3,11}$	$a_{3,12}$	$a_{3,13}$	$a_{3,14}$	$a_{3,15}$	$a_{3,16}$	$a_{3,17}$
$(2,1,\frac{1}{2},-\frac{1}{2})$	0	0	0	$a_{4,4}$	0	0	0	$a_{4,9}$	$a_{4,10}$	$a_{4,11}$	$a_{4,12}$	$a_{4,13}$	$a_{4,14}$	$a_{4,15}$	$a_{4,16}$	$a_{4,17}$
$(2,1,\frac{3}{2},\frac{3}{2})$	0	0	0	0	$a_{5,5}$	0	0	$a_{5,9}$	$a_{5,10}$	$a_{5,11}$	$a_{5,12}$	$a_{5,13}$	$a_{5,14}$	$a_{5,15}$	$a_{5,16}$	$a_{5,17}$
$(2,1,\frac{3}{2},\frac{1}{2})$	0	0	0	0	0	$a_{6,6}$	0	$a_{6,9}$	$a_{6,10}$	$a_{6,11}$	$a_{6,12}$	$a_{6,13}$	$a_{6,14}$	$a_{6,15}$	$a_{6,16}$	$a_{6,17}$
$(2,1,\frac{3}{2},-\frac{1}{2})$	0	0	0	0	0	0	$a_{7,7}$	$a_{7,9}$	$a_{7,10}$	$a_{7,11}$	$a_{7,12}$	$a_{7,13}$	$a_{7,14}$	$a_{7,15}$	$a_{7,16}$	$a_{7,17}$
$(2,1,\frac{3}{2},-\frac{3}{2})$	0	0	0	0	0	0	0	$a_{8,8}$	$a_{8,9}$	$a_{8,10}$	$a_{8,11}$	$a_{8,12}$	$a_{8,13}$	$a_{8,14}$	$a_{8,15}$	$a_{8,16}$
$(2,0,\frac{1}{2},\frac{1}{2})$	$a_{1,9}^*$	$a_{2,9}^*$	$a_{3,9}^*$	$a_{4,9}^*$	$a_{5,9}^*$	$a_{6,9}^*$	$a_{7,9}^*$	$a_{8,9}^*$	$a_{9,9}$	0	0	0	0	0	0	0
$(2,0,\frac{1}{2},-\frac{1}{2})$	$a_{1,10}^*$	$a_{2,10}^*$	$a_{3,10}^*$	$a_{4,10}^*$	$a_{5,10}^*$	$a_{6,10}^*$	$a_{7,10}^*$	$a_{8,10}^*$	0	$a_{10,10}$	0	0	0	0	0	0
$(2,1,\frac{1}{2},\frac{1}{2})$	$a_{1,11}^*$	$a_{2,11}^*$	$a_{3,11}^*$	$a_{4,11}^*$	$a_{5,11}^*$	$a_{6,11}^*$	$a_{7,11}^*$	$a_{8,11}^*$	0	0	$a_{11,11}$	0	0	0	0	0
$(2,1,\frac{1}{2},-\frac{1}{2})$	$a_{1,12}^*$	$a_{2,12}^*$	$a_{3,12}^*$	$a_{4,12}^*$	$a_{5,12}^*$	$a_{6,12}^*$	$a_{7,12}^*$	$a_{8,12}^*$	0	0	0	$a_{12,12}$	0	0	0	0
$(2,1,\frac{3}{2},\frac{3}{2})$	$a_{1,13}^*$	$a_{2,13}^*$	$a_{3,13}^*$	$a_{4,13}^*$	$a_{5,13}^*$	$a_{6,13}^*$	$a_{7,13}^*$	$a_{8,13}^*$	0	0	0	0	$a_{13,13}$	0	0	0
$(2,1,\frac{3}{2},\frac{1}{2})$	$a_{1,14}^*$	$a_{2,14}^*$	$a_{3,14}^*$	$a_{4,14}^*$	$a_{5,14}^*$	$a_{6,14}^*$	$a_{7,14}^*$	$a_{8,14}^*$	0	0	0	0	0	$a_{14,14}$	0	0
$(2,1,\frac{3}{2},-\frac{1}{2})$	$a_{1,15}^*$	$a_{2,15}^*$	$a_{3,15}^*$	$a_{4,15}^*$	$a_{5,15}^*$	$a_{6,15}^*$	$a_{7,15}^*$	$a_{8,15}^*$	0	0	0	0	0	0	$a_{15,15}$	0
$(2,1,\frac{3}{2},-\frac{3}{2})$	$a_{1,16}^*$	$a_{2,16}^*$	$a_{3,16}^*$	$a_{4,16}^*$	$a_{5,16}^*$	$a_{6,16}^*$	$a_{7,16}^*$	$a_{8,16}^*$	0	0	0	0	0	0	0	$a_{16,16}$

where

$$a_{1,1} = \varepsilon_{20\frac{1}{2}} + \Delta\varepsilon_{20\frac{1}{2}\frac{1}{2}}$$

$$a_{1,9} = e^{ik_x \frac{a}{\sqrt{3}}} \left[\varepsilon_{20\frac{1}{2}} S \left(20\frac{1}{2}, 20\frac{1}{2} \right)_{\frac{1}{2}} + K \left(20\frac{1}{2}, 20\frac{1}{2} \right)_{\frac{1}{2}} \right] \\ + e^{-ik_x \frac{a}{2\sqrt{3}} + ik_y \frac{a}{2}} \left[\varepsilon_{20\frac{1}{2}} S \left(20\frac{1}{2}, 20\frac{1}{2} \right)_{\frac{1}{2}} + K \left(20\frac{1}{2}, 20\frac{1}{2} \right)_{\frac{1}{2}} \right] \\ + e^{-ik_x \frac{a}{2\sqrt{3}} - ik_y \frac{a}{2}} \left[\varepsilon_{20\frac{1}{2}} S \left(20\frac{1}{2}, 20\frac{1}{2} \right)_{\frac{1}{2}} + K \left(20\frac{1}{2}, 20\frac{1}{2} \right)_{\frac{1}{2}} \right]$$

$$a_{1,10} = 0$$

$$a_{1,11} = 0$$

and so on...

Table 4: Overlap matrix representation in tabular form.

\times	A								B							
	$(2,0,\frac{1}{2},\frac{1}{2})$	$(2,0,\frac{1}{2},-\frac{1}{2})$	$(2,1,\frac{1}{2},\frac{1}{2})$	$(2,1,\frac{1}{2},-\frac{1}{2})$	$(2,1,\frac{3}{2},\frac{3}{2})$	$(2,1,\frac{3}{2},\frac{1}{2})$	$(2,1,\frac{3}{2},-\frac{1}{2})$	$(2,1,\frac{3}{2},-\frac{3}{2})$	$(2,0,\frac{1}{2},\frac{1}{2})$	$(2,0,\frac{1}{2},-\frac{1}{2})$	$(2,1,\frac{1}{2},\frac{1}{2})$	$(2,1,\frac{1}{2},-\frac{1}{2})$	$(2,1,\frac{3}{2},\frac{3}{2})$	$(2,1,\frac{3}{2},\frac{1}{2})$	$(2,1,\frac{3}{2},-\frac{1}{2})$	$(2,1,\frac{3}{2},-\frac{3}{2})$
$(2,0,\frac{1}{2},\frac{1}{2})$	1	0	0	0	0	0	0	0	$b_{1,9}$	$b_{1,10}$	$b_{1,11}$	$b_{1,12}$	$b_{1,13}$	$b_{1,14}$	$b_{1,15}$	$b_{1,16}$
$(2,0,\frac{1}{2},-\frac{1}{2})$	0	1	0	0	0	0	0	0	$b_{2,9}$	$b_{2,10}$	$b_{2,11}$	$b_{2,12}$	$b_{2,13}$	$b_{2,14}$	$b_{2,15}$	$b_{2,16}$
$(2,1,\frac{1}{2},\frac{1}{2})$	0	0	1	0	0	0	0	0	$b_{3,9}$	$b_{3,10}$	$b_{3,11}$	$b_{3,12}$	$b_{3,13}$	$b_{3,14}$	$b_{3,15}$	$b_{3,16}$
$(2,1,\frac{1}{2},-\frac{1}{2})$	0	0	0	1	0	0	0	0	$b_{4,9}$	$b_{4,10}$	$b_{4,11}$	$b_{4,12}$	$b_{4,13}$	$b_{4,14}$	$b_{4,15}$	$b_{4,16}$
$(2,1,\frac{3}{2},\frac{3}{2})$	0	0	0	0	1	0	0	0	$b_{5,9}$	$b_{5,10}$	$b_{5,11}$	$b_{5,12}$	$b_{5,13}$	$b_{5,14}$	$b_{5,15}$	$b_{5,16}$
$(2,1,\frac{3}{2},\frac{1}{2})$	0	0	0	0	0	1	0	0	$b_{6,9}$	$b_{6,10}$	$b_{6,11}$	$b_{6,12}$	$b_{6,13}$	$b_{6,14}$	$b_{6,15}$	$b_{6,16}$
$(2,1,\frac{3}{2},-\frac{1}{2})$	0	0	0	0	0	0	1	0	$b_{7,9}$	$b_{7,10}$	$b_{7,11}$	$b_{7,12}$	$b_{7,13}$	$b_{7,14}$	$b_{7,15}$	$b_{7,16}$
$(2,1,\frac{3}{2},-\frac{3}{2})$	0	0	0	0	0	0	0	1	$b_{8,9}$	$b_{8,10}$	$b_{8,11}$	$b_{8,12}$	$b_{8,13}$	$b_{8,14}$	$b_{8,15}$	$b_{8,16}$
$(2,0,\frac{1}{2},\frac{1}{2})$	$b_{1,9}^*$	$b_{2,9}^*$	$b_{3,9}^*$	$b_{4,9}^*$	$b_{5,9}^*$	$b_{6,9}^*$	$b_{7,9}^*$	$b_{8,9}^*$	1	0	0	0	0	0	0	0
$(2,0,\frac{1}{2},-\frac{1}{2})$	$b_{1,10}^*$	$b_{2,10}^*$	$b_{3,10}^*$	$b_{4,10}^*$	$b_{5,10}^*$	$b_{6,10}^*$	$b_{7,10}^*$	$b_{8,10}^*$	0	1	0	0	0	0	0	0
$(2,1,\frac{1}{2},\frac{1}{2})$	$b_{1,11}^*$	$b_{2,11}^*$	$b_{3,11}^*$	$b_{4,11}^*$	$b_{5,11}^*$	$b_{6,11}^*$	$b_{7,11}^*$	$b_{8,11}^*$	0	0	1	0	0	0	0	0
$(2,1,\frac{1}{2},-\frac{1}{2})$	$b_{1,12}^*$	$b_{2,12}^*$	$b_{3,12}^*$	$b_{4,12}^*$	$b_{5,12}^*$	$b_{6,12}^*$	$b_{7,12}^*$	$b_{8,12}^*$	0	0	0	1	0	0	0	0
$(2,1,\frac{3}{2},\frac{3}{2})$	$b_{1,13}^*$	$b_{2,13}^*$	$b_{3,13}^*$	$b_{4,13}^*$	$b_{5,13}^*$	$b_{6,13}^*$	$b_{7,13}^*$	$b_{8,13}^*$	0	0	0	0	1	0	0	0
$(2,1,\frac{3}{2},\frac{1}{2})$	$b_{1,14}^*$	$b_{2,14}^*$	$b_{3,14}^*$	$b_{4,14}^*$	$b_{5,14}^*$	$b_{6,14}^*$	$b_{7,14}^*$	$b_{8,14}^*$	0	0	0	0	0	1	0	0
$(2,1,\frac{3}{2},-\frac{1}{2})$	$b_{1,15}^*$	$b_{2,15}^*$	$b_{3,15}^*$	$b_{4,15}^*$	$b_{5,15}^*$	$b_{6,15}^*$	$b_{7,15}^*$	$b_{8,15}^*$	0	0	0	0	0	0	1	0
$(2,1,\frac{3}{2},-\frac{3}{2})$	$b_{1,16}^*$	$b_{2,16}^*$	$b_{3,16}^*$	$b_{4,16}^*$	$b_{5,16}^*$	$b_{6,16}^*$	$b_{7,16}^*$	$b_{8,16}^*$	0	0	0	0	0	0	0	1

where

$$b_{1,9} = e^{ik_x \frac{a}{\sqrt{3}}} S \left(20 \frac{1}{2}, 20 \frac{1}{2} \right)_{\frac{1}{2}} + e^{-ik_x \frac{a}{2\sqrt{3}} + ik_y \frac{a}{2}} S \left(20 \frac{1}{2}, 20 \frac{1}{2} \right)_{\frac{1}{2}} + e^{-ik_x \frac{a}{2\sqrt{3}} - ik_y \frac{a}{2}} S \left(20 \frac{1}{2}, 20 \frac{1}{2} \right)_{\frac{1}{2}}$$

$$b_{1,10} = 0$$

$$b_{1,11} = 0$$

$$\begin{aligned} b_{1,12} = & e^{ik_x \frac{a}{\sqrt{3}}} S \left(20 \frac{1}{2}, 21 \frac{1}{2} \right)_{\frac{1}{2}} \\ & + e^{-ik_x \frac{a}{2\sqrt{3}} + ik_y \frac{a}{2}} \left[\left(-\frac{1}{2} - i \frac{\sqrt{3}}{2} \right) S \left(20 \frac{1}{2}, 21 \frac{1}{2} \right)_{\frac{1}{2}} \right] \\ & + e^{-ik_x \frac{a}{2\sqrt{3}} - ik_y \frac{a}{2}} \left[\left(-\frac{1}{2} + i \frac{\sqrt{3}}{2} \right) S \left(20 \frac{1}{2}, 21 \frac{1}{2} \right)_{\frac{1}{2}} \right] \end{aligned}$$

and so on...

References

- [1] K. Higuchi, D. B. Hamal, and M. Higuchi, “Relativistic tight-binding approximation method for materials immersed in a uniform magnetic field: Application to crystalline silicon,” *Phys. Rev. B*, vol. 91, p. 075122, Feb 2015.
- [2] K. S. Novoselov, A. K. Geim, S. V. Morozov, D. Jiang, M. I. Katsnelson, I. Grigorieva, S. Dubonos, Firsov, and AA, “Two-dimensional gas of massless dirac fermions in graphene,” *nature*, vol. 438, no. 7065, pp. 197–200, 2005.
- [3] A. Bostwick, T. Ohta, T. Seyller, K. Horn, and E. Rotenberg, “Quasiparticle dynamics in graphene,” *Nature physics*, vol. 3, no. 1, pp. 36–40, 2007.
- [4] A. H. Castro Neto, F. Guinea, N. M. R. Peres, K. S. Novoselov, and A. K. Geim, “The electronic properties of graphene,” *Rev. Mod. Phys.*, vol. 81, pp. 109–162, Jan 2009.
- [5] S. Chen, M. He, Y.-H. Zhang, V. Hsieh, Z. Fei, K. Watanabe, T. Taniguchi, D. H. Cobden, X. Xu, C. R. Dean, *et al.*, “Electrically tunable correlated and topological states in twisted monolayer–bilayer graphene,” *Nature Physics*, vol. 17, no. 3, pp. 374–380, 2021.
- [6] M. Fan, J. Wu, J. Yuan, L. Deng, N. Zhong, L. He, J. Cui, Z. Wang, S. K. Behera, C. Zhang, *et al.*, “Doping nanoscale graphene domains improves magnetism in hexagonal boron nitride,” *Advanced Materials*, vol. 31, no. 12, p. 1805778, 2019.
- [7] Y. Zheng and T. Ando, “Hall conductivity of a two-dimensional graphite system,” *Phys. Rev. B*, vol. 65, p. 245420, Jun 2002.
- [8] A. K. Geim and K. S. Novoselov, “The rise of graphene,” in *Nanoscience and technology: a collection of reviews from nature journals*, pp. 11–19, World Scientific, 2010.
- [9] S. G. Sharapov, V. P. Gusynin, and H. Beck, “Magnetic oscillations in planar systems with the dirac-like spectrum of quasiparticle excitations,” *Phys. Rev. B*, vol. 69, p. 075104, Feb 2004.
- [10] Y. Gao, S. A. Yang, and Q. Niu, “Geometrical effects in orbital magnetic susceptibility,” *Phys. Rev. B*, vol. 91, p. 214405, Jun 2015.
- [11] R. Kundu, “Tight-binding parameters for graphene,” *Modern Physics Letters B*, vol. 25, no. 03, pp. 163–173, 2011.
- [12] S. Reich, J. Maultzsch, C. Thomsen, and P. Ordejón, “Tight-binding description of graphene,” *Phys. Rev. B*, vol. 66, p. 035412, Jul 2002.
- [13] R. Roldán, M. P. López-Sancho, and F. Guinea, “Effect of electron-electron interaction on the fermi surface topology of doped graphene,” *Phys. Rev. B*, vol. 77, p. 115410, Mar 2008.

- [14] D. D. Koelling and G. O. Arbman, “Use of energy derivative of the radial solution in an augmented plane wave method: application to copper,” *Journal of Physics F: Metal Physics*, vol. 5, pp. 2041–2054, nov 1975.
- [15] T. Takeda, “The scalar relativistic approximation,” *Zeitschrift für Physik B Condensed Matter*, vol. 32, no. 1, pp. 43–48, 1978.
- [16] M. Higuchi and A. Hasegawa, “Self-consistent relativistic linear augmented planewave method: Application to y b g a 2,” *Journal of the Physical Society of Japan*, vol. 64, no. 3, pp. 830–847, 1995.
- [17] M. Higuchi and A. Hasegawa, “Fermi surface of ceru 2 within local-density functional theory,” *Journal of the Physical Society of Japan*, vol. 65, no. 5, pp. 1302–1311, 1996.
- [18] D. B. Hamal, M. Higuchi, and K. Higuchi, “Calculation of magnetic oscillations via the magnetic-field-containing relativistic tight-binding approximation method: Revisiting the de haas–van alphen effect,” *Phys. Rev. B*, vol. 91, p. 245101, Jun 2015.
- [19] M. Gmitra, S. Konschuh, C. Ertler, C. Ambrosch-Draxl, and J. Fabian, “Band-structure topologies of graphene: Spin-orbit coupling effects from first principles,” *Phys. Rev. B*, vol. 80, p. 235431, Dec 2009.
- [20] L. I. Schiff, *Quantum Mechanics*. McGRAW-HILL BOOK COMPANY, INC., 1955.
- [21] P. Hohenberg and W. Kohn, “Inhomogeneous electron gas,” *Phys. Rev.*, vol. 136, pp. B864–B871, Nov 1964.
- [22] W. Kohn and L. J. Sham, “Self-consistent equations including exchange and correlation effects,” *Phys. Rev.*, vol. 140, pp. A1133–A1138, Nov 1965.
- [23] M. Higuchi, D. B. Hamal, A. Shrestha, and K. Higuchi, “Reduced effective g-factor in graphene,” *Journal of the Physical Society of Japan*, vol. 88, no. 9, p. 094707, 2019.